

A Novel Approach for Predicting Frictional Factor during Fluid Flow In well Tubings and Flowlines.

Akinade Akinwumi, Omohimoria Charles

Abstract - One of the main challenges facing by production engineers is the ability to choose an accurate friction factor during a fluid flow, it was observed that most of the existing models (Fanning, 1944), Blasius, 1914) and moody e.t.c) over-predict the values of frictional factors when compare with the experimental value, this is due to the fact that these models are dependent on Reynolds number and pipe roughness, and since pipe roughness changes with use, this make them inaccurate, it is therefore important to develop a new correlation that will be a function of Reynolds number and that can accurately matched with experimental data in order to aid accurate prediction of wax deposition and thickness during crude oil production. In this research work an accurate frictional factor model (correlation) was developed by considering the universal velocity profile (distribution) over the cross section of a pipe during the lamina and turbulent flow, the model result was tested and validated with complex cases.

Keywords: Friction factor, Reynold number, Velocity profile, Laminar flow

1. INTRODUCTION

The basis for the application of Wax thickness model starts from the development of Friction factor as a function of Reynolds number, due to the result published by Wax Joint Industry Project (Wax JIP) sponsored by US Department of Energy, the research work was carried out at the University of Tulsa. It was published that wax interface can be assumed smooth, since a significant amount of oil is usually trapped in the wax layer. This smooth wax interface was confirmed by observation of the wax layer in a spool piece removed from the Wax JIP single phase flowline during a preliminary test. Therefore the friction factor models can be developed by considering the velocity profile distribution in a laminar and turbulent flow pipe, from which friction factor as a function of Reynolds number will be developed for both laminar and turbulent flow.

In general there are three types of fluid flow in pipes; laminar, turbulent and transitional flow. Laminar flow generally happens when dealing with small pipes, low flow velocities and with highly viscous fluids. At low velocities fluids tend to flow without lateral mixing, and adjacent layers slide past one another like playing cards. There are neither cross currents nor eddies. Laminar flow can be regarded as a series of liquid cylinders in the pipe, where the innermost parts flow the fastest, and the cylinder touching the pipe isn't

moving at all. In turbulent flow, the fluid moves erratically in the form of cross currents and eddies. Turbulent flow happens in general at high flow rates and with larger pipes. Transitional flow is a mixture of laminar and turbulent flow, with turbulence in the center of the pipe, and laminar flow near the edges.

It has long been known that in turbulent flow a rough pipe leads to a larger friction factor for a given Reynolds number than a smooth pipe does. If a rough pipe is smoothed, the friction factor is reduced. When further smoothing brings about no further reduction in friction factor for a given Reynolds number, the tube is said to be hydraulically smooth.

In turbulent flow, the friction factor, f depends upon the Reynolds number and on the relative roughness of the pipe, k/D , where, k is the roughness parameter (average roughness height of the pipe) and D is the inner diameter of the pipe. The general behavior of turbulent pipe flow in the presence of surface roughness is well established. When k is very small compared to the pipe diameter D i.e. $k/D \rightarrow 0$, f depends only on N_{Re} . When k/D is of a significant value, at low N_{Re} , the flow can be considered as in smooth regime (there is no effect of roughness). As N_{Re} increases, the flow becomes transitionally rough, called as transition regime in which the friction factor rises above the smooth value and is a function of both k and N_{Re} and as N_{Re} increases more and more, the flow eventually reaches a fully rough regime in which f is independent of N_{Re} .

In a smooth pipe flow, the viscous sub layer completely submerges the effect of k on the flow. In this case, the friction factor f is a function of N_{Re} and is independent of the effect of k on the flow. In case of rough pipe flow, the viscous sub layer thickness is very small when compared to roughness height and thus the flow is dominated by the roughness of the pipe

• Akinade Akinwumi is currently a PhD student of University of Ibadan, Nigeria. PH-08038090006. E-mail: akinchem2003@yahoo.com

• Omohimoria Charles is currently a lecturer at Petroleum Engineering department of Afe Babalola University, Ado-Ekiti, Nigeria. He is currently a PhD student of University of Ibadan. PH: 08035851646 E-mail: charles_4real@yahoo.com

wall and f is the function only of k/D and is independent of N_{Re}

It has been observed that most of the deposition models that were developed by earlier researchers over predict the location and rate of wax build up in flowlines when compared with experimental results, this is as a results of their derivation from a faulty thermodynamic principles (or models), it is therefore imperative to develop a viable and reliable deposition model that can accurately predict wax deposition rate in flowlines when compared with experimental data by using an accurate friction factor during modeling of such equation. One of the main challenges facing by production engineers is the ability to choose an accurate friction factor during a fluid flow, it was observed that most of the existing models (Fanning(1944), Blasius (1914) and moody e.t.c) over-predict the values of frictional factors when compare with the experimental value, this is due to the fact that these models are dependent on Reynolds number and pipe roughness, and since pipe roughness changes with use, this makes them inaccurate, it is therefore important to develop a new correlation that will be a function of Reynolds number and that can accurately matched with experimental data in order to aid accurate prediction of wax deposition and thickness during crude oil production.

In this research work an accurate frictional factor model (correlation) was developed by considering the universal velocity profile (distribution) over the cross section of a pipe during the lamina and turbulent flow, the model results was validated by subjecting it to a complex flow situations.

2.0 MODEL FORMULATION

One of the main challenges facing by production engineers is the ability to choose an accurate friction factor during a fluid flow, it was observed that most of the existing models (Fanning(1944), Blasius (1914) and moody e.t.c) over-predict the values of frictional factors when compare with the experimental value, this is due to the fact that these models are dependent on Reynolds number and pipe roughness, and since pipe roughness changes with use, this makes them inaccurate, it is therefore important to develop a new correlation that will be a function of Reynolds number and that can accurately matched with experimental data in order to aid accurate prediction of wax thickness in flowline.

(A) MODEL DEVELOPMENT

This can be achieved by consideration of universal velocity profile (distribution) over the cross section of a pipe during the lamina and turbulent flow

FOR LAMINAR FLOW

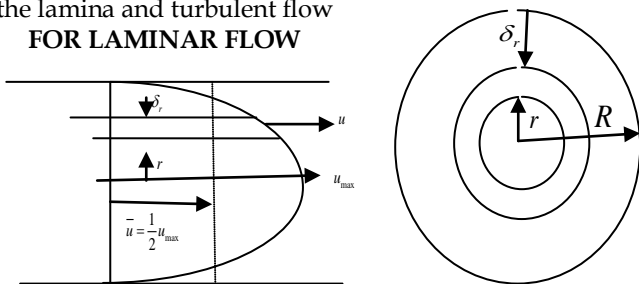


Fig 3.2: Velocity distribution in laminar flow pipe

To calculate the volume flow rate through a pipe of diameter d in term of a pressure drop over a length L we apply:

Poiseuille Equation

$$Q = \frac{\Delta P \pi d^4}{128 \mu L} \tag{1}$$

but head loss due to friction is given as

$$h_f = \frac{\Delta P}{\rho g} \tag{2}$$

$$= \frac{128 \mu L Q}{\rho g} \tag{3}$$

now:

$$Q = \pi \left(\frac{d^4}{4} \right) u \tag{4}$$

applying Darcy equation for head loss in circular pipe

$$h_f = \frac{128 \mu L \pi d^2 u}{4 \rho g \pi d^4} = \frac{4 \phi L u^2}{2 g d} \tag{5}$$

or

$$\phi = \left(\frac{128 \mu}{16 \rho u d} \right) \tag{6}$$

recall that

$$R_e = \frac{\rho \mu d}{\mu} \tag{7}$$

Substitute into equation 6

$$\phi = \frac{8}{R_e} \tag{8}$$

$$\phi = 8 R_e^{-1} \tag{8}$$

The above equation is plotted as a straight line on log-log plot and is independent of surface roughness.

FOR TURBULENT FLOW

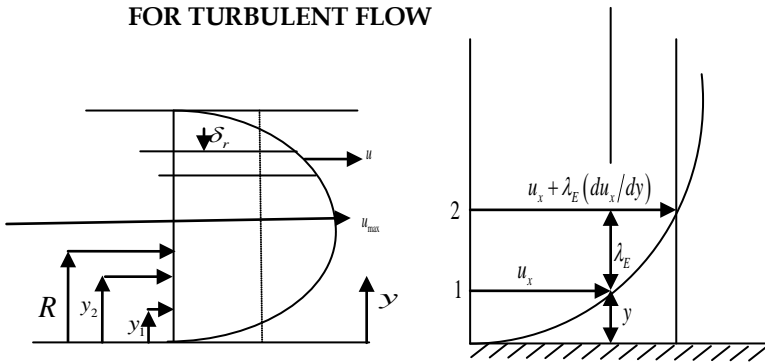


Fig 3.3a: Velocity distribution in turbulent flow pipe
 Fig 3.3b: Prandtl mixing length

Fig 3.3b above shows the velocity profile near a surface.

At point 1, the velocity is u_x and at point 2 the velocity is u_x^1 . For an eddy velocity u_{Ey} in the direction perpendicular to the surface, the fluid is transported away from the surface at a mass rate per unit area equal to $u_{Ey} \rho$, this fluid must be replaced by an equal mass of fluid which is transferred in the opposite direction. The momentum transferred away from the surface per unit time is given as

$$R_y = \rho u_{Ey} (u_x - u_x^1) \quad (9)$$

If the distance between the two location is approximately equal to the mixing length λ_E , and if the velocity gradient is nearly constant over the distance

$$\frac{u_x^1 - u_x}{\lambda_E} \approx \frac{du_x}{dy} \quad (10)$$

Assuming again that $u_x^1 - u_x \approx u_{Ey}$

$$R = \rho \lambda_E^2 \left(\frac{du_x}{dy} \right)^2 \quad (11)$$

it is assumed throughout that no mixing take place with the intervening fluid when eddy transport fluid element over a distance equal to the mixing length close to the surface $R_y \rightarrow R_0$,

and

$$\sqrt{\frac{R}{\rho}} = \lambda_E \frac{du_x}{dy} \quad (12)$$

$\sqrt{\frac{R}{\rho}}$ is known as shearing stress velocity of frictional velocity and it is usually denoted by u^* . In steady state flow over a plane surface, or close to the wall for flow in a pipe, u^* is constant and equation 3.37 can be integrated provided that the relation between λ_E and y is known. λ_E will increase with y and, if a linear relationship is assumed then

$$\lambda_E = k y \quad (13)$$

$$u^* = k \frac{du_x}{dy} \quad (14)$$

On integration

$$\frac{u_x}{u^*} = \left(\frac{1}{k} \right) \ln \left(\frac{y u^* \rho}{\mu} \right) + B \quad (15)$$

Where B is a constant.

$$\text{Or } \frac{u_x}{u^*} = \left(\frac{1}{k} \right) \ln \left(\frac{y u^* \rho}{\mu} \right) + B^1 \quad (16)$$

Since $\frac{u^* \rho}{\mu}$ is a constant, B^1 will also be constant.

Writing the dimensionless velocity term $\frac{u_x}{u^*} = u^+$

and the dimensionless derivatives as

$$\left(\frac{y u^* \rho}{\mu} \right) y = y^+$$

$$u^+ = \frac{1}{k} \ln y^+ + B^1 \quad (17)$$

if equation 7 is applied to the outer edge of the boundary layer, when $y = \delta$ (boundary layer thickness) and $u_x = u_s$ (stream velocity) then:

$$\frac{u_s}{u^*} = \frac{1}{k} \ln \frac{\delta u^* \rho}{\mu} + B^1 \quad (18)$$

Subtracting equation (16) from (18)

$$\frac{u_s - u_x}{u^*} = \frac{1}{k} \ln \frac{\delta}{y} \quad (19)$$

Using experimental result results for flow of fluid over both smooth and rough surfaces Nikurade found K to have a value of 0.4

Thus:

$$\frac{u_s - u_x}{u^*} = 2.5 \ln \frac{\delta}{y} \quad (20)$$

For fully developed flow in pipe $\delta = r$ and u_s is the velocity at the axis and then

$$\frac{u_s - u_x}{u^*} = 2.5 \ln \frac{r}{y} \quad (21)$$

equation 4.36 is known as velocity defect law. Note that for turbulent core the value of 0.4 can be substituted for in equation 3.42 to give:

$$u^+ = 2.5 \ln y^+ + B^1 \quad (22)$$

From the plot of u^+ and y^+ . It is observed that for a smooth surface $B^1 = 5.5$. Thus for a smooth pipe $u^+ = 2.5 \ln y^+ + 5.5$

Substituting for $u^+ = \frac{u_s}{u^*}$ and $y^+ = \frac{r \rho u^*}{\mu}$ into

equation 3.47

$$\text{Thus: } u_s = u^* \left(2.5 \ln \frac{r \rho u^*}{\mu} + 5.5 \right) \quad (24)$$

but it also necessary to obtain expression for mean velocity U of the fluid, we use the relation

$$u = \int_0^r \frac{(2\pi(r-y) dy u_x)}{\pi r^2} \quad (25)$$

$$= 2 \int_0^1 u_x \left(1 - \frac{y}{r} \right) d \left(\frac{y}{r} \right) \quad (26)$$

Substituting for u_x equation 3.50

$$u = 2 \int_0^1 \left(u_x + 2.5 u^* \ln \frac{r}{y} \right) \left(1 - \frac{y}{r} \right) d \left(\frac{y}{r} \right) \quad (27)$$

$$\frac{u}{u_s} = 2 \int_0^1 \left(u_x + 2.5 \frac{u^*}{u_s} \ln \frac{y}{r} \right) \left(1 - \frac{y}{r} \right) d \left(\frac{y}{r} \right) \quad (28)$$

$$= 2 \left\{ \frac{y}{r} - \frac{1}{2} \left(\frac{y}{r} \right)^2 \right\}_0^1 + 5.0 \frac{u^*}{u_s} \left\{ \left(\ln \frac{y}{r} \right) \left[\frac{y}{r} - \frac{1}{2} \left(\frac{y}{r} \right)^2 \right] \right\}_0^1$$

$$- \int_0^1 \left(\frac{y}{r} \right)^{-1} \left[\frac{y}{r} - \frac{1}{2} \left(\frac{y}{r} \right)^2 \right] d \left(\frac{y}{r} \right) \quad (30)$$

$$= 1 + 5.0 \frac{u^*}{u_s} \left\{ 0 - \left(\frac{y}{r} \right) - \frac{1}{4} \left(\frac{y}{r} \right)^2 \right\}_0^1 \quad (31)$$

$$= 1 + 5 \frac{u^*}{u_s} \left(-\frac{3}{4} \right) = 1 - 3.75 \left(\frac{u^*}{u_s} \right) \quad (32)$$

Substituting into equation (24)

$$u = 3.75 u^* = u^* \left\{ 2.5 \ln \left[\left(\frac{d \rho u}{\mu} \right) \left(\frac{r}{d} \right) \left(\frac{u^*}{u} \right) \right] + 5.5 \right\} \quad (33)$$

Since $R_e = \frac{d \rho u}{\mu} = \frac{u_{\max}}{u}$ when $r = d$

$$u + 3.75 u^* = u^* (5.5)$$

$$u + 3.75 u^* = 5.5 u^* \quad (34)$$

Dividing through by u^*

$$\frac{u}{u^*} = 5.5 - 3.75 \tag{35}$$

Since $\frac{u}{u^*} = R_e \phi^4$

Therefore

$$R_e \phi^4 = 1.75 \tag{36}$$

$$\phi^4 = \left(\frac{1.75}{R_e} \right)^{\frac{1}{4}}$$

Therefore $\phi = 0.0396 R_e^{-\frac{1}{4}}$.

Finally,

$$\phi = 0.0396 R_e^{-0.25} \tag{37}$$

Comparing equation (8) and (37), that is

$\phi = 8 R_e^{-1}$ For laminar flow

$\phi = 0.0396 R_e^{-\frac{1}{4}}$ For turbulent flow

We can come out with a combined model for our predicted friction factor

$$\phi = x R_e^{-y} \tag{38}$$

Where

$x = 8$ and $y = 1$ for laminar flow

$x = 0.0396$ and $y = 0.25$ for turbulent flow

results are tabulated in Table 4.4 and shown pictorially in Figure 4.3

TABLE 4.4: Comparison between Friction factor for Model output and experimental data

REYNOLDS NO	EXPERIMENTAL DATA	MODEL RESULTS
2500	0.00522	0.0056
3000	0.00525	0.00535
4000	0.00475	0.00498
5000	0.0045	0.00471
6000	0.00425	0.0045
7000	0.004	0.00433
8000	0.003875	0.00419
9000	0.00375	0.00407
10000	0.003625	0.00396
20000	0.00325	0.00333
30000	0.00275	0.00301
40000	0.002625	0.0028
50000	0.0025	0.00265
60000	0.002375	0.00253
70000	0.00225	0.00243
80000	0.0021875	0.00235
90000	0.002125	0.00229
100000	0.0020625	0.00223
200000	0.00185	0.00187
300000	0.00165	0.00169
400000	0.00155	0.00157
500000	0.00145	0.00149
600000	0.0014	0.00142
700000	0.00135	0.00137
800000	0.00132	0.00132
900000	0.00128	0.00129
1000000	0.00123	0.00125

3.0 MODEL VALIDATION

The model results is then compared with an experimental values obtained from the work of H.S. Fogler et al. (2000) the

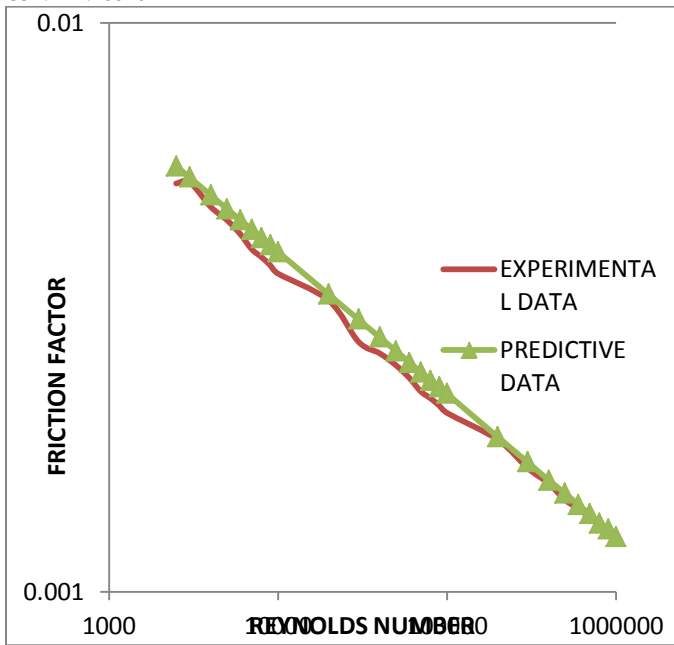


Fig 4.3: Comparison between Friction Factor of Experimental Data and Model Results

Moreover the Friction factor model output for turbulent flow (equation 3.60) is further validated by comparison with smooth pipe equation for turbulent flow of the other existing research work derived by Fanning, Blasius or Moody. The results are presented in the Table 4.4 and Figure 4.4 below.

TABLE 4.5: Comparison of Model output with other existing models (Fanning & Blasius)

RENOLD NO	EXPERIMENTAL DATA	MODEL RESULT	FARNNING FRICTION FACTOR	BLASIUS FRICTION FACTOR
2500	0.00522	0.0056	0.0112	
3000	0.00525	0.00535	0.0107	0.0427
4000	0.00475	0.00498	0.00993	0.0397
5000	0.0045	0.00471	0.0094	0.0376
6000	0.00425	0.0045	0.00898	0.036
7000	0.004	0.00433	0.00864	0.0345
8000	0.003875	0.00419	0.00835	0.0334
9000	0.00375	0.00407	0.00811	0.0324
10000	0.003625	0.00396	0.0079	0.0316
20000	0.00325	0.00333	0.00664	0.0266
30000	0.00275	0.00301	0.006	0.024
40000	0.002625	0.0028	0.00559	0.0223
50000	0.0025	0.00265	0.00528	0.0211
60000	0.002375	0.00253	0.00505	0.0202
70000	0.00225	0.00243	0.00486	0.0194
80000	0.0021875	0.00235	0.0047	0.0188
90000	0.002125	0.00229	0.00456	0.0182
100000	0.0020625	0.00223	0.00444	0.0178
200000	0.00185	0.00187	0.00374	0.0149
300000	0.00165	0.00169	0.00338	0.0135
400000	0.00155	0.00157	0.00314	0.0126
500000	0.00145	0.00149	0.00297	0.0119

600000	0.0014	0.00142	0.00284	0.0114
700000	0.00135	0.00137	0.00273	0.0109
800000	0.00132	0.00132	0.00264	0.0106
900000	0.00128	0.00129	0.00256	0.0103
1x10 ⁶	0.00123	0.00125	0.0025	0.00999

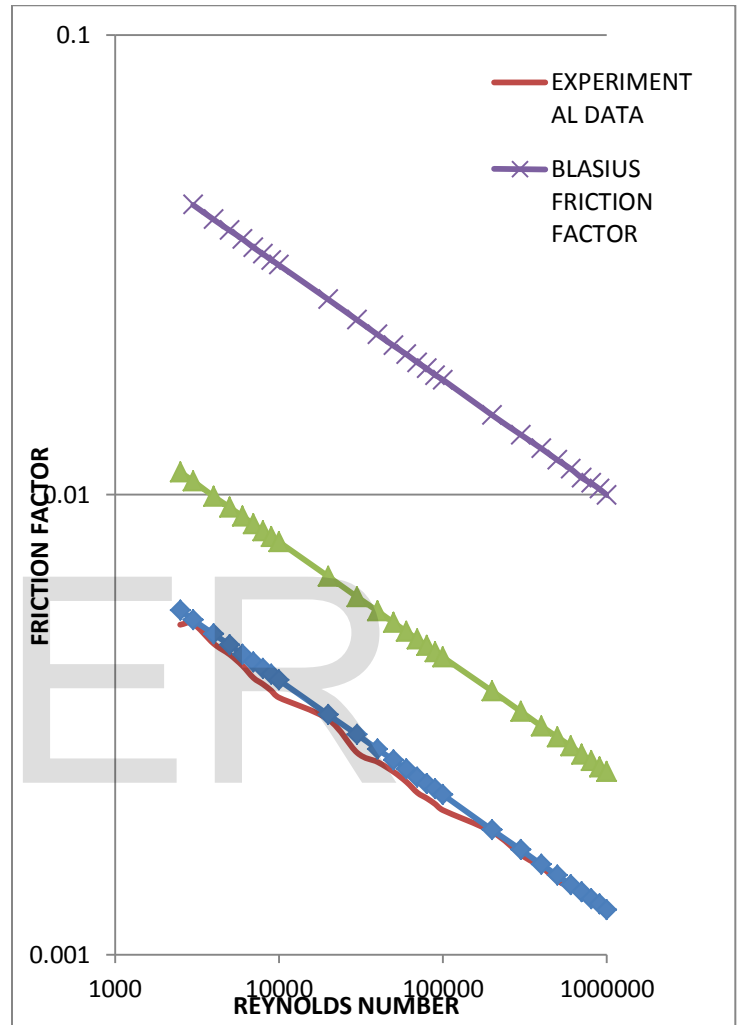


Fig 4.4: Comparison between Model output, Experimental data and other existing Models (Blasius and Fanning)

4.0 DISSCUSSION OF RESULT

The results of the model were compared with those obtained experimentally in Table 4.4; this is also shown graphically in Figure 4.3. It can be seen that the model output is in agreement with experimental result. The maximum absolute deviation was in the range of 0.00038, which in other word confirm the accuracy of the newly developed model.

The accuracy of the friction factor of the model output is further tested by comparison with friction factor for a smooth pipe of the other existing model as seen in Table 4.5, it can be seen in Figure 4.4 that there is a wide deviation between the other existing model and experimental value, where as there is

close agreement between model output and experimental data, which confirm the accuracy of modeling a friction factor from velocity distribution profile in a flow pipe.

5.0 CONCLUSION

The approach employed in this work is easily accessible since the application requires constant thermodynamic data (properties that varies with temp) and rheological properties of the crude.

The following conclusion can be deduced from this research work.

1. An accuracy modeling of a friction factor from velocity distribution profile in a flow pipe as been established
2. A friction factor model that is a function of surface roughness has been established.

REFERENCES

- [1] Jorder R. M. " Paraffin Deposition and Prevention in oil wells" Journal of Technology, Trans AIME, Vol 237, pg 1605-1612, December, 1966.
- [2] K. S. Pedersen, P. Skovborg, H. P. Rønningsen: 'Wax Precipitation from North Sea Crude Oils. 4. Thermodynamic Modelling', Energy & Fuels, 5, 924, (1991).
- [3] K. S. Pedersen: 'Prediction of Cloud Point Temperatures and Amount of Wax Precipitated' SPE 27629.
- [4] K. W. Won: 'Thermodynamic Calculation of Cloud Point Temperatures and Wax Phase Compositions of Refined Hydrocarbon Mixtures', Fluid Phase Equil., 53, 377, (1989).
- [5] Kaufman D. S., Port Arthur, "control of wax deposition", United State Patent Office, 2364222, Dec., 5 1944.
- [6] Keating J.F., R.A. Wattenbarger, "The simulation of Paraffin Deposition and Removal in Wellbores", SPE 27871, Western Regional Meeting, Long Beach - California, March (1994)
- [7] Leontaritis K. J., Leontaritis J. D. "Cloud Point and Wax Measurement Techniques" SPE 80267, 2003.
- [8] Majeed, A., Bringedal, B., and Overra, S.: "Model to Calculate Wax Deposition for North Sea Oils" Oil and Gas Journal (June 1990) 63-69.
- [9] Mansoori, G.A. and Jiang, T. S.: "Asphaltene Deposition and Its Role in Enhanced Oil Recovery Miscible Gas Flooding," presented at the 3rd European Conference on EOR, Rome, Italy, April 1985.
- [10] Patton, C. C.: "Relation of Adsorption of High Molecular Weight Petroleum Fractions to Paraffin Deposition", PhD Dissertation, The U. of Texas (Jan., 1964).
- [11] Perry, R. H., Green D.W. Perry's Chemical Engineers' handbook. Mc Graw-Hall, New York, 50th edition, 1992.
- [12] Richardson and Coulson, Chemical Engineering, Butterworth Heinemann, Jordan hill, Oxford, sixth edition, chapter 3 & 6, pg 58-140, published 2000.
- [13] Svendsen J.A., "Mathematical Modeling of Wax Deposition in Oil Pipeline Systems", AIChE Journal, August (1993).
- [14] Svendsen, J. A. "Mathematical Modeling of Wax Deposition in Oil Pipeline System." AIChE Journal, 39: 1377-1388, 1993.
- [15] T. G. Monger-McClure, J. E. Tackett, L. S. Merrill: 'Deep Star Comparisons of Cloud Point Measurement & Paraffin Prediction Methods', SPE 38774.
- [16] T. S. Brown, V. G. Niesen, D. D. Erickson: 'Measurement and Prediction of the Kinetics of Paraffin Deposition', SPE 26548.